POLITECNICO DI TORINO
Repository ISTITUZIONALE

3D printing of PBAT-based composites filled with agro-wastes via selective laser sintering

(Article begins on next page)

27 June 2024

ELSEVIER

3D printing of PBAT-based composites filled with agro-wastes via selective laser sintering

Giovanna Colucci [a,b,*], Federico Lupone [a], Federica Bondioli [a,b], Massimo Messori [a,b]

[a] *Politecnico di Torino, Department of Applied Science and Technology (DISAT), Corso Duca degli Abruzzi 24, 10129 Torino, Italy*
[b] *National Interuniversity Consortium of Materials Science and Technology (INSTM), Via G. Giusti 9, 50121 Firenze, Italy*

ARTICLE INFO

ABSTRACT

Nowadays, biodegradable polymeric materials can play a key role in many fields, including food packaging and biomedical. In the present work, composite powders based on PBAT matrix were prepared by mixing spherical particles obtained by emulsion solvent process with two different biofillers coming from food agro-wastes: a corn by-product and a filler derived from wine production. Sustainable PBAT-based composites were then successfully realized for the first time by means of selective laser sintering (SLS). This paper combines the use of natural fillers within a biodegradable matrix and 3D printing process. Fillers and composite powders were completely characterized as well as the PBAT-based composites obtained by SLS. The effect of biofillers within the PBAT matrix was investigated, by means of TGA, DSC, SEM, and DMA analyses. The bio-based composites obtained by SLS showed increased complex structures. Regarding the processability the printed samples are characterized by a good level of dimensional accuracy and porosity. Thus, biomedical field could benefit from the use of these kinds of fully biodegradable PBAT-based composites.

1. Introduction

The growing interest in biodegradable polymers, due to the drastic environmental issues derived from the use of traditional polymers, drives industrial and academic researchers towards the development of innovative and more sustainable polymeric materials [1–4].

Generally, biodegradable polymers are divided into two classes: natural polymers and synthetic polymers. Natural polymers are obtained directly from nature, like chitosan [3,4], whereas the second category includes biodegradable polymers coming from fossil sources, like poly (butylene adipate-co-terephthalate) (PBAT) [5–9].

PBAT is a thermoplastic polyester, deriving from petroleum resources. It is a flexible, not harmful, and totally biodegradable polymer, with mechanical properties comparable to those of low-density polyethylene (LDPE). The properties of PBAT make it a very promising environmentally friendly material for many applications fields, such as biomedical devices, agricultural, and food packaging [10–12]. However, the high production costs, compared with the classical polymers, limit its use making its biodegradability advantageous only if strictly required. The addition of natural fillers is reported in literature as a valid alternative to develop PBAT-based composites with performances that

could match or, in some cases, exceed that of the most used polymers [13–20], decreasing the material cost and ensuring the total biodegradability of the material. Clearly, the mechanical properties of the biofillers-reinforced composites vary depending on their composition, chemical properties, and morphology (particles or fibres) [12–20].

The effect of the addition of fillers, such as rice husk, corn husk, tea leaves, banana peels, and coconut shell on the final properties of several polymeric matrices are widely reported in literature [16,17]. The composites were prepared by using different main methods: in-situ polymerization, melt mixing, and solvent casting [13]. Regarding PBAT matrix, many authors focused their investigations on the addition of different fillers, such as lignin [14], microcrystalline cellulose [15,20], and coffee grounds [19] to PBAT with the aim to enhance the final properties and to valorize industrial or agricultural wastes, leading to the preparation of totally biodegradable composites. Therefore, the reinforcement of a flexible polymer, like PBAT, allows to modify the viscoelastic and mechanical properties of the polymeric material with the final purpose to enlarge its application in the food packaging, thanks to the similarity of PBAT performances with LDPE [10,11,20].

In the present study, the advantages of the use of biofillers, coming from agro-wastes, within a biodegradable matrix such as PBAT, were

---

combined with the advantages of additive manufacturing (AM) [21–29]. Specifically, the novelty introduced with this paper was the preparation, for the first time, of fully biodegradable PBAT-based composite powders to be used to print by selective laser sintering (SLS) bulk samples with complex geometry.

SLS is considered the most booming AM technique for polymer processing because it assures to obtain parts with high geometrical accuracy and surface quality, and to realize parts with good level of complexity and flexibility, without the need of support structures or post-processing [30–32].

Considering that the powder quality significantly affects the final performance of the 3D printed components, the powder design and preparation are of crucial importance for this technology, also considering the limited number of thermoplastic polymeric powders available [29–31]. For this reason, the polymer powder should be as spherical as possible to encourage free-flowing characteristics. Moreover, powders should have a particle size lower than 100 μm and good flowability during spreading, which are strictly dependent on the particle shape and size distribution [32–34]. Thus, PBAT powders were firstly prepared following an emulsion solvent evaporation/precipitation method, as previously reported [34]. Subsequently, PBTA powders mixed with different biofillers deriving from agro-wastes, were used to print different geometries by SLS. According to the authors' best knowledge, the preparation of PBAT-based composites containing agro-wastes by SLS 3D printer is a novel study not already reported in the literature. This study can be considered a successive step with respect to the previous paper regarding PBAT powder production [34]. The main difference lies in the addition of biofillers powders within the PBAT matrix in order to prepare fully biodegradable composites reducing the use of the pure polymeric matrix and valorising the wastes of agriculture and food production. The agro-wastes can act as low-cost materials and natural reinforcing agents for the PBAT matrix, maintaining the biodegradability characteristic of the starting polymer [23]. A wide characterization of the PBAT-based composites was performed to correlate processability, morphology, thermal, and mechanical properties of the final composites. Preliminary tests were also carried out to investigate the cytocompatibility of the novel PBAT-based composites.

2. Materials and methods

2.1. Materials

Poly (butylene adipate-*co*-terephthalate) (PBAT) was acquired by MAIP Group. Poly (vinyl alcohol) (PVA) and chloroform were acquired from Merck. Two different biofillers were used to prepare the composites: a yellow filler derived from Italian corn germ meal by-products, named GTF, (density of 1.44 g/cm^3) and a grey powder coming from Italian wine by-products, named WPL-DH, (density of 1.69 g/cm^3) kindly supplied by Agromateriae (Agromateriae srl, Faenza, Ravenna, Italy). The biofillers were put in oven at 80 °C for 3 h, according to the recommendation reported in the supplier datasheets.

2.2. PBAT-based composites preparation

The PBAT powder was obtained by emulsion solvent evaporation/precipitation method, following the procedure described in a previously published work [34]. Bio-based composites were prepared by adding two powders of biofillers, coming from agro-food wastes, to the PBAT polymeric powder, at different weight percentages, 5 and 10 wt% respectively, and by mixing them for 2 h in a Turbula® T2F shaker mixer (WAB Group).

2.3. SLS process

The PBAT-based composites were obtained by using a Sharebot SnowWhite[2] machine (Sharebot S.r.l., Nibionno, Varese, Italy). The powders were distributed onto the print bed and selectively melted by the laser beam in air atmosphere. The building chamber temperature was set at around 63 °C for PBAT parts and 65 °C for the composites. Moreover, the laser scan speed was kept at 2400 mm/s for the infill region and 3840 mm/s for the border of all the 3D printed parts. Finally, the thickness of each layer was set to 0.1 mm. The process parameters were optimized by trial-and-error experiments based on the previous experimental study on neat PBAT [34].

2.4. Characterization methods

2.4.1. Morphology

The morphology of the PBAT powder and the two biofillers was firstly studied by using a Phenom™ XL G2 Scanning Electron Microscope (Thermo Fisher Scientific, USA) with a voltage of 15 kV. The samples were previously sputter-coated with gold for 3 min, at 10^{-3} mbar and 10 mA current flow. Each specimen of PBAT-based composite was fractured in liquid nitrogen and the fracture surface was analyzed after metallization with platinum for 15 s. The micrographs were recorded at different magnification for each powder and each bio-based composite.

2.4.2. Particle size distribution (PSD)

The particle size distribution of the two biofillers was analyzed by using a Morphology 4 automated analyzer (Malvern Panalytical, Malvern, UK). The measurements were performed according to the procedure previously reported [34].

2.4.3. Density tests

The density of PBAT and biofillers powders was measured using an Ultrapyc 5000 pycnometer (Anton Paar GmbH, Graz, Austria) using helium, according to the ASTM B923-20 standard. Three tests were carried out for each sample at 20 °C.

The density of PBAT-based composites was evaluated through the Archimedes' method in accordance with ASTM B962–17 standard. This method is non-destructive and consists in calculating the density of the sample by measuring its mass in air and in ethanol (ρ_{liq} = 0.789 g/cm^3).

The density values of the samples were evaluated taking into account the closed porosity or the total porosity (open and closed) using Equation (1) and Equation (2) respectively:

$$\rho_{closed} = \frac{W_{air} \times \rho_{liq}}{(W_{air} - W_{liq})} \tag{1}$$

$$\rho = \frac{W_{air} \times \rho_{liq}}{(W_{fin} - W_{liq})} \tag{2}$$

where W_{air} and W_{liq} are the weights in grams of the sample measured in air and in ethanol, and W_{fin} is the final weight of the sample measured in air after drying, and ρ_{liq} the density of ethanol. Subsequently, the closed and total porosity of the printed samples were calculated, by using the Equation (3) and Equation (4) respectively:

$$\Phi closed = \left(1 - \frac{\rho_{closed}}{\rho_{powder}}\right) \times 100 \tag{3}$$

$$\Phi = \left(1 - \frac{\rho}{\rho_{powder}}\right) \times 100 \tag{4}$$

where ρ_{powder} is the neat polymeric powder density for PBAT parts or the density of each composite containing the biofillers for bio-based composite parts. In the latter case the density is calculated by using the "rule of mixtures" reported in Equation (5).

$$\rho_{powder} = \rho_f \bullet V_f + \rho_m \bullet V_m \tag{5}$$

where ρ_f is the density of the filler, ρ_m is the matrix density, V_f is the

filler volume fraction, and V_m is the polymeric volume fraction.

2.4.4. Rheological analysis

A parallel plate rotational rheometer (AR 2000, TA Instruments, New Castle, DE, USA) was adopted to study the melt viscosity of the neat PBAT and its bio-based composites reinforced with GTF and WPL-DH fillers at different weight percentages. The rheometer consists of two electrically heated plates with diameter of 25 mm, rotating between each other to apply a controlled stress or strain to a molten sample. Prior to testing, the powders were dried in oven for 24 h at 50 °C and cylindrical samples (diameter and thickness of 1 mm and 25 mm respectively) were produced by compression molding using the following parameters: temperature of 150 °C, pressure of 100 MPa and cycle time of 3 min. The melt viscosity of PBAT and PBAT-based composites was evaluated through a frequency sweep test (from $0.1 \, s^{-1}$ to $100 \, s^{-1}$) with a strain amplitude of 20 % at a temperature of 150 °C. This temperature was chosen since it is slightly above the melting endset of both PBAT and bio-based composites powders, as shown by DSC analysis, thus lying within the temperature range of interest for SLS processing. The distance between the plates was set at 1000 μm for all tests.

2.4.5. Thermogravimetric analysis (TGA)

TGA analyses on PBAT and on the composites reinforced with biofillers were evaluated by using a Mettler-Toledo TGA 851e instrument (Mettler Toledo, Columbus, Ohio, USA). The experiments were performed in air from room temperature to 800 °C, at a heating rate of 10 °C/min. The TGA curves were normalized to the mass of the specimens, and the first derivative curves determined on their relative thermograms.

2.4.6. Differential scanning calorimetry (DSC)

Differential scanning calorimetry (DSC) measurements were performed using a DSC 214 Polyma Equipment (Netzsch Group, Germany), under nitrogen flow by performing two heating scans from −50 °C to 250 °C, and one cooling scan from 250 °C to − 50 °C, with a heating and cooling rate of 10 °C/min. The thermal transitions were evaluated on the cooling and the second heating cycles. The Equation (6) was used for the degree of crystallinity (X_c) evaluation:

$$X_c(\%) = \frac{\Delta H_m}{\Delta H_{mPBAT}^0 * X_{PBAT}} \times 100 \qquad (6)$$

where, ΔH_m is the melting enthalpy of the samples, X_{PBAT} the weight fraction of PBAT in the biobased composite, and ΔH_{mPBAT}^0 the 100 % crystalline PBAT melting enthalpy (114 J/g), respectively [20,34]. The phase transitions were also assessed to determine the sintering window of the polymeric matrix for SLS processing, well-known from literature [31,34].

2.4.7. Dynamic mechanical analysis (DMA)

The viscoelastic properties of the 3D printed PBAT-based samples were evaluated with a Triton Technology Instrument. The tests were carried out from −80 °C to 80 °C in liquid nitrogen, in tensile configuration at 1 Hz of frequency and 3 °C/min of heating rate. The dimensions of rectangular printed samples were 50x10x2. The elastic (E') modulus of PBAT matrix and the relative composites, and the glass transition temperature (T_g), as maximum of tan δ curve were determined.

2.4.8. Cytocompatibility

Indirect cytotoxicity tests were performed following the ISO10933-5 guidelines, to recognize any cytotoxic events resulting from the release of compounds from the PBAT polymer matrix and the PBAT-based composites filled with the two agro-wastes. Briefly, 0.1 g of the 3D printed samples were soaked into 1 mL of complete medium (Dulbecco's Modified Eagle's Medium, 15 % fetal bovine serum, 1 % penicillin streptomycin) for 24 h obtaining conditioned medium. Human

fibroblasts (HFF-1 ATCC® cells) were cultured in a 96-plate multiwell at 2×10^4 cells/well (n = 6 samples for each condition). After 24 h, culture medium was removed from each well and replaced with conditioned medium while control samples (CTRL) were obtained by substituting the medium with HFF-1 fresh medium. After 24 h, medium was replaced with 100 μL of medium containing CellTiter-Blue® (Promega) reagent. After 1 h of incubation at 37 °C, 100 μL were placed in a black 96-well plate and cell viability was detected by measuring the fluorescence at 590 nm using SYNERGYTM HTX multimode plate reader (BioTeK, Winooski, VM, USA). Cell viability was calculated as a percent of the CNTR.

3. Results and discussion

3.1. Powders characterization

The PBAT powder and biofillers morphology was studied by SEM analysis, by acquiring micrographs at different magnifications, as reported in Fig. 1. As visible from Fig. 1 (a), PBAT particles, prepared by emulsion solvent evaporation/precipitation method, show typical spherical shape and a particle size lower than 80 μm, in accordance with the characteristics of powders useful for SLS processing [31–34].

Moreover, SEM images reported in Fig. 1 evidence the morphologies of the two different biofillers, GTF (b) and WPL-DH (c), respectively, which are characterized by a reasonably well-defined structure with irregular shape particles, short length, and surface roughness. GTF powder is characterized by a quasi-spherical tiny flake morphology (b), while WPL-DH has a completely different morphology given by the random alternation of small and coarse-grain particles (c) probably due to the presence of a mix of grape skin, seeds, and stalks. The biofillers seem to have irregular particle sizes varying from few micrometres to thirty micrometres, as visible from SEM micrographs.

The obtained results were reported in Fig. 2 (a) and (b) for GTF and Fig. 2 (c) and (d) for WPL-DH, respectively. The granulometric analyses underline that the PSD of the GTF filler is about 7.5 μm with circularity values located in the range between 0.89 and 0.93, to confirm the quasi-spherical morphology of the flakes of the filler derived from corn-wastes, as seen in Fig. 2 (a-b). Therefore, Fig. 2 (c-d) report a broader filler distribution of the WPL-DH particles, centered at around 8.5 μm, with an average circularity of the wine wastes particles approximately close to 0.89, due to irregular particles geometry, as previously seen from SEM images of Fig. 1.

The PSD results evidence that the fillers particles size distribution and shape are not ideal for SLS. In fact, it requires spherical particles with size lower than 100 μm. As clearly reported in literature, the flowability of polymeric powders is strictly influenced by specific particles geometries. For example, particles in form of flakes can led to final components with very high porosity in SLS process [21]. Therefore, although the addition of biofillers, deriving from wastes of the agricultural food processing industry, is a suitable way for enhancing the final polymers performance, the characteristic fillers morphology can represent a critical aspect during the printing process [12–22].

The powders density was evaluated by gas pycnometry. As a result, the average true density was estimated as 1.24 g/cm³ for PBAT powder, 1.42 g/cm³ for GTF, and 1.68 g/cm³ for WPL-DH, respectively, which agrees with the theoretical values reported in the suppliers' datasheets. Finally, the two biofillers were characterized from thermal stability point of view, by means of TGA analysis performed in air. Fig. 3 reports the thermograms (a) and their relative first derivative curves (b) for both types of biofillers, GTF (red curve) and WPL-DH (blue curve), respectively.

As evident from the plots relative to the TG measurements, the two biofillers show very different thermal behaviors. In fact, both show a first peak at low temperatures, 60 °C for GTF and 70 °C for WPL-DH respectively, probably due to the presence of traces of water eventually absorbed on the particles surface. The organic fraction of GTF starts
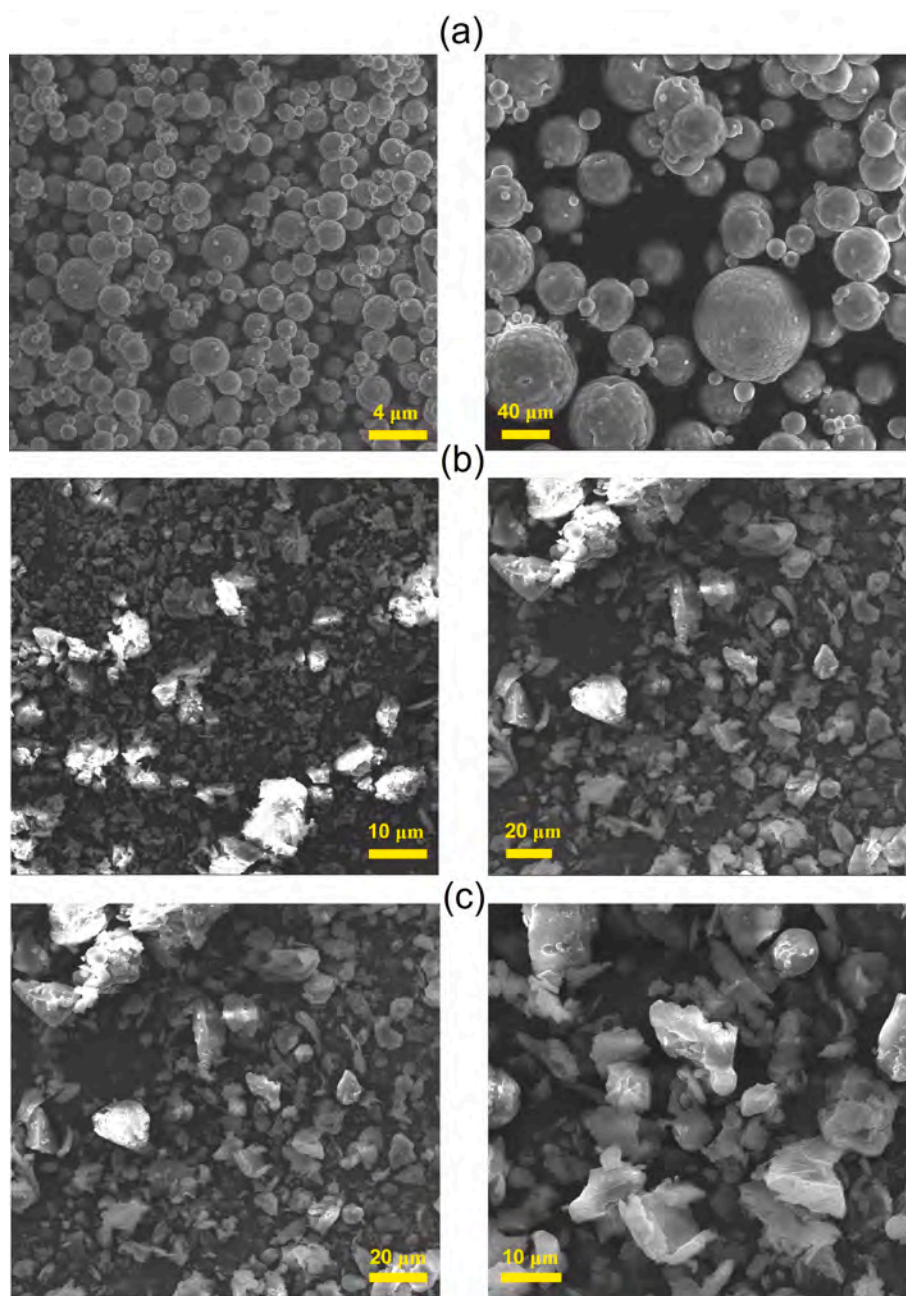
Fig. 1. Morphology of the neat PBAT powder (a), corn waste GTF (b), and wine waste WPL-DH (c), respectively,zfor the bio-based composites preparation.

to thermally degrade at 286 °C where the main degradation peak appears, followed by a second degradation peak at 447 °C, and a third peak at higher temperature (667 °C). On the contrary, the WPL-DH powder shows a very broad degradation pattern. The filler decomposition begins at 306 °C and ends at 520 °C. Moreover, from Fig. 3 it is possible to see another significant difference in the thermal behavior of the two biofillers used in this work. GTF contains a higher organic content with respect to WPL-DH filler, as underlined by the 6 wt% of residue found at 800 °C for the corn waste, respect to the higher in residue content of 42 wt% found for the wine wastes at the same temperature. This difference is surely due to the different composition and origin of the two kinds of biofillers. In fact, if GTF is a yellow powder obtained by maize by-products, WPL-DH is a grey powder derived from winemaking by-products, such as grape skin, seeds, and stalks, which can contain inorganic components explaining the presence of the high value of residue at 800 °C.

3.2. Rheological properties of PBAT powders

Understanding the rheological behavior of the polymeric powders is crucial for designing 3D printing materials useful for SLS applications because their rheology directly impacts their printability. Rheological analysis was performed to evaluate the melt viscosity of PBAT and PBAT-based composites, which can affect the flow behavior through the 3D printing system ensuring successful printing and high-quality printed parts [34,35]. The variation of the complex viscosity as a function of shear rate at a temperature of 150 °C is shown in Fig. 4.

This temperature is of great interest because it is about 10 °C higher than the melting endset of both neat PBAT and PBAT-based composites. In fact, during SLS processing the coalescence of the polymeric powders takes place when the temperature rises just above the melting point due to the action of the laser.

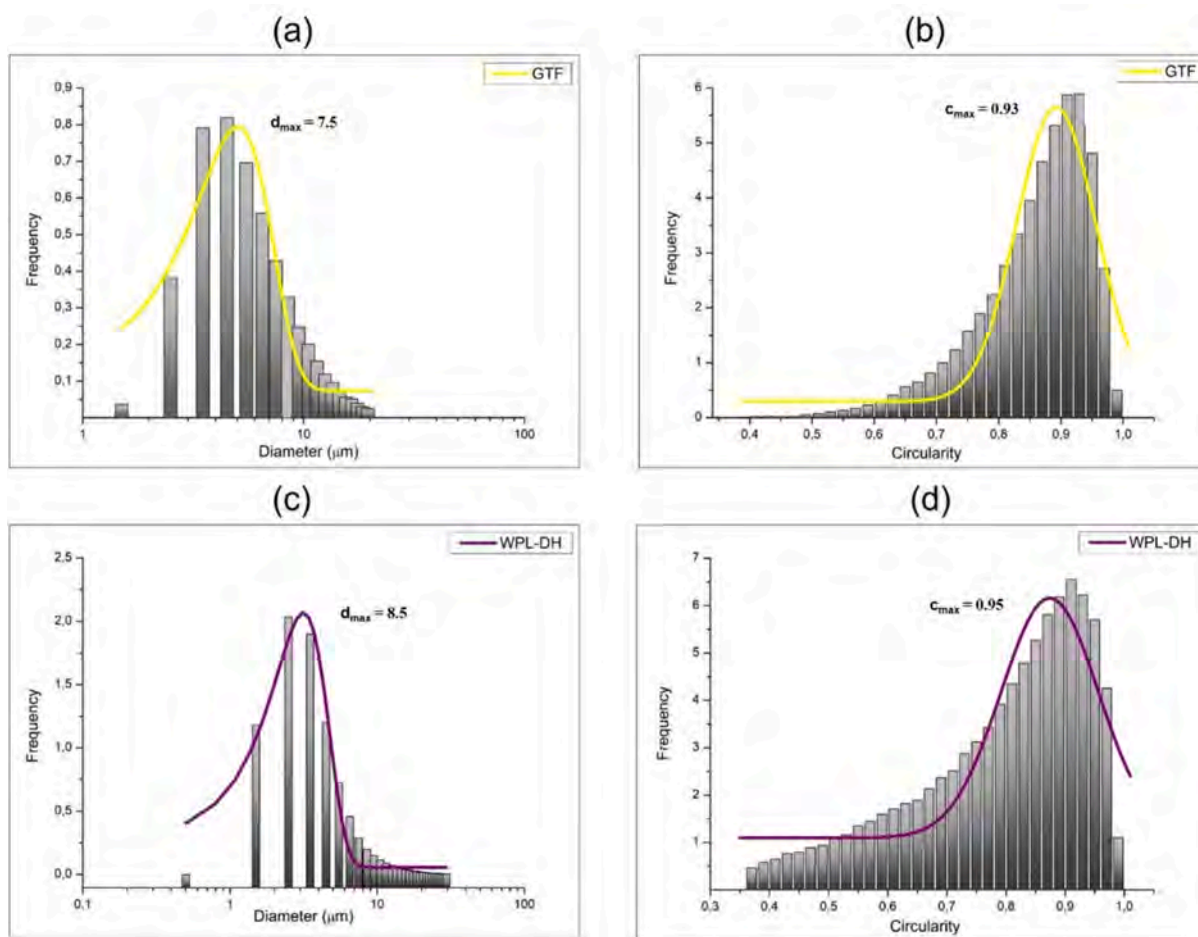Moreover, the identification of a Newtonian plateau at low shear

Fig. 2. PSD and circularity of the biofillers, GTF (a-b) and WPL-DH (c-d).
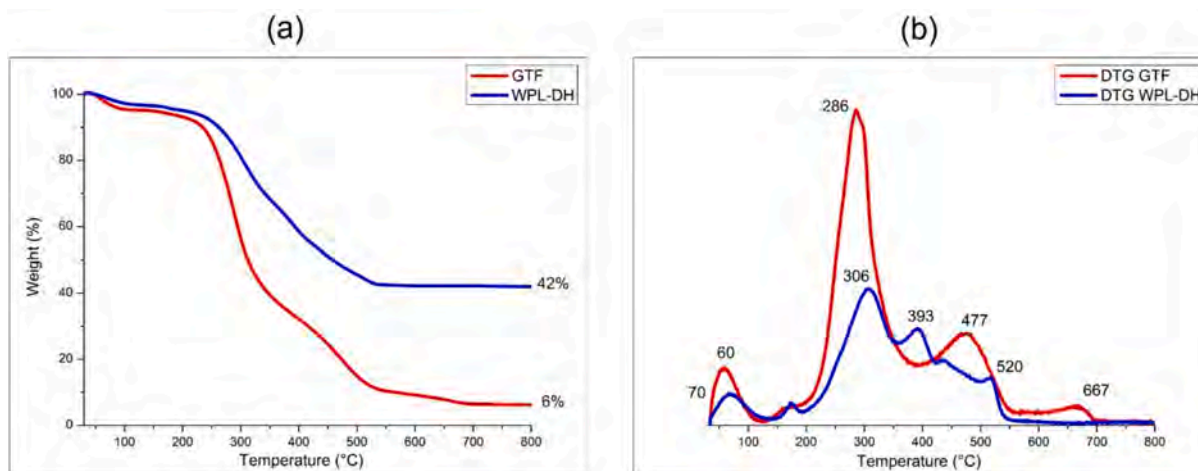

Fig. 3. TGA curves (a) and first derivative curves (b), performed in air, of the biofillers, GTF and WPL-DH.

rates (i.e., viscosity tending to a constant value (η_0) at vanishing shear rate), is highly favorable for laser sintering because no shear stresses are applied during the process [36].

The bi-logarithmic plot shows that PBAT powders exhibit a nearly Newtonian behavior at very low shear rate (i.e., < 0.2 s^{-1}) followed by shear thinning at moderate to high shear rates Fig. 4 (a). In this case, since a Newtonian plateau seems to develop at shear rate lower than 0.2 s^{-1} (black arrow in Fig. 4 (a)), the zero-shear viscosity (η_0) can be

reasonably extrapolated at shear rate equal to 0.1 s^{-1}, corresponding to a value around 4300 Pa·s. The PBAT-based composites show similar shear thinning behavior at moderate to high shear rates compared to the neat polymer. By contrast, the low frequency region exhibits a slight increase in the complex viscosity as the shear rate decreases, indicating a non-Newtonian behavior (red arrow in Fig. 4 (b)).

It is worth noting that the bio-based composites display significantly higher viscosities compared to the neat polymer in the entire shear rates
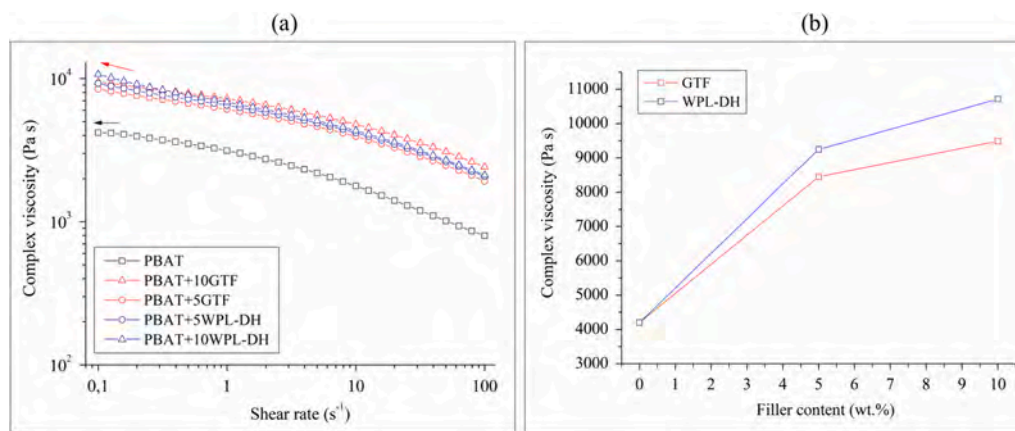
Fig. 4. Rheological data for neat PBAT and PBAT-based composites reinforced with GTF and WPL-DH fillers: (a) complex viscosity curves as a function of shear rate and (b) effect of bio-fillers content on viscosity at very low shear rate ($0.1 \ s^{-1}$).

range, while the differences between bio-fillers themselves (i.e., GTF and WPL-DH) as well as between different filler content (i.e., 5 wt% and 10 wt%) are relatively small, as visible in Fig. 4 (a). The different rheological behavior observed for neat PBAT, and its PBAT-based composites is related to the presence of the solid bio-fillers, which interfere with the relaxation dynamics of polymeric chains by modifying their relaxation mechanisms as well as by hindering their movements [37]. This phenomenon is probably responsible for the apparent yield stress behavior recorded at low shear rates and the marked increase of viscosity values in the entire range of shear rates investigated (Fig. 4 (a)).

The increase of viscosity as a function of bio-fillers content is clearly shown in Fig. 4 (b), where the values of viscosity at low shear rates (0.1 s^{-1}) are plotted since they are more representative of the real processing conditions during laser sintering. The addition of WPL-DH leads to a higher increment of viscosity compared to GTF, as shown in Fig. 4 (b), thus explaining the lower densification of PBAT + WPL-DH printed parts (Table 1). The same observation can be applied to justify the lower density and mechanical performances of the composites reinforced with the higher percentage of bio-fillers (10 wt%) with respect to the 5 wt% counterparts (Table 1 and Table 3).

For all materials the viscosities are higher compared to 10^3 Pa s, which is the threshold value for obtaining almost fully-dense parts realized by SLS [36]. These high viscosity values (Fig. 4) could explain the relatively poor densification of neat PBAT, and its bio-composites printed parts.

This finding can be attribute to the biofillers presence which leads to a significant increase of the degree of porosity, which strongly affects the final resolution of the 3D printed parts in terms of structural integrity and surface finish, compromising the overall quality of the final printed object [34,35]. However, although the definition of an ideal viscosity range for SLS polymeric powders is still object of discussion among the researchers, a wide number of publications suggest that, for semi-crystalline polymers like PBAT, higher viscosity values are acceptable too for those applications where a high level of porosities is strictly desired [34–37]. In fact, the high pore content of the PBAT-based

Table 2
DSC data of 3D printed specimens.

Sample	T_m [°C]	ΔH_m (J/g)	X_c (%)	T_c (°C)	T_g (°C)
PBAT	120	13.6	12	68	−30
PBAT + 5GTF	122	14.1	13	64	−30
PBAT + 10GTF	122	24.4	24	64	−30
PBAT + 5WPL-DH	120	14.8	14	67	−30
PBAT + 10WPL-DH	122	15.7	15	67	−30

Table 3
DMA data, at −40 °C, of 3D printed PBAT specimens and PBAT-based composites.

Sample	E' [MPa]	E'' [MPa]	T_g [°C]
PBAT	153	3.7	−17
PBAT + 5GTF	150	5.5	−16
PBAT + 10GTF	110	4.4	−15
PBAT + 5WPL-DH	224	5.5	−17
PBAT + 10WPL-DH	149	3.9	−16

composites could be highly favorable for fabricating functional 3D parts in energy and biomedical fields (e.g., scaffolds, electrodes, membranes for filtering).

3.3. SLS printing of bio-based PBAT composites

Preliminary tests were carried out before the printing process to reach the best compromise between the laser power, the building chamber temperature, the laser scan speed, and the powder flowability to select the optimal printing parameters for obtaining by SLS the desired three-dimensional PBAT-based composites.

Several printing tests were performed by changing the laser power and the scanning speed to optimize the energy absorption, melting, and sintering of the powder bed. As well-known, higher laser power and slower scanning speeds can be useful to improve the melting between the powder's particles, but they can also increase the risk of overheating and surface roughness [28–34]. Moreover, other tests were done to optimize the bed temperature and the build chamber conditions to ensure uniform heating and cooling, minimizing thermal gradients and reducing warping and residual stresses in the final 3D printed part.

Fig. 5 presents some representative printed components prepared by adding the two biofillers wastes to the PBAT powder. The pictures of Fig. 5 (a) report a flexible snowflake made of 22 layers of powder deposition, a rigid honeycomb hexagonal prism made of 40 layers, and a
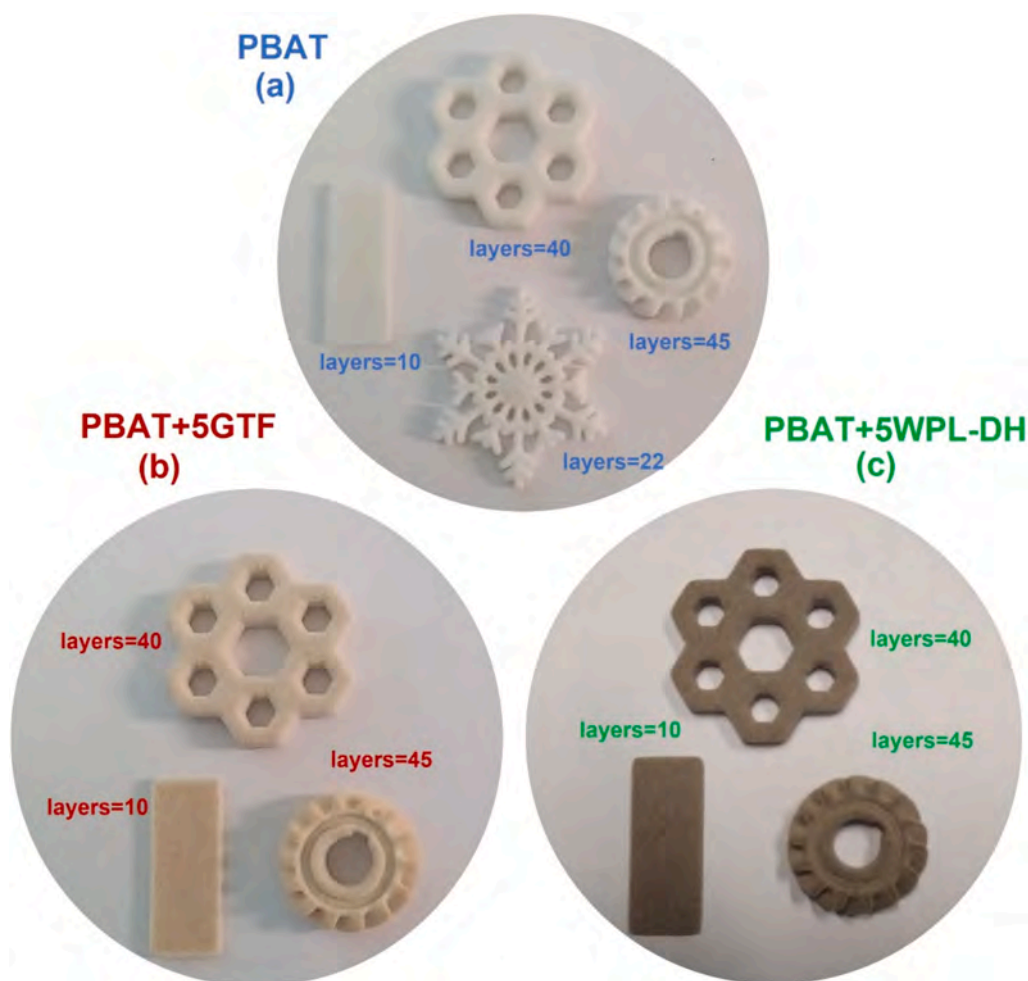
Table 1
Porosity values of printed PBAT specimens and PBAT-based composites.

Sample	ρ_{closed} [g/cm³]	ρ [g/cm³]	ϕ [%]
PBAT	1.18	0.60	52
PBAT + 5GTF	1.22	0.62	56
PBAT + 10GTF	1.22	0.60	58
PBAT + 5WPL-DH	1.19	0.66	61
PBAT + 10WPL-DH	1.21	0.63	62

Fig. 5. Some representative photographs of 3D printed parts of pure PBAT (a) compared with specimens containing 5 wt% of GTF (b) and WPL-DH (c), respectively.

gearwheel made of 45 layers of powder, obtained using the neat PBAT powder. Moreover, it is also possible to see, from the pictures of Fig. 5, an overview of the objects realized by depositing layer by layer the PBAT powder filled with 5 wt% of GTF (b), and of WPL-DH (c), representing a simple rectangle, a honeycomb hexagonal prism, and a gearwheel.

The samples of the polymer and the PBAT-based composites are characterized by a good level of details, without significant visible defects. No post-printing procedures were done, except the removal of the excess of powder on the sample's surfaces. The printed specimens show high dimensional accuracy. However, they also reveal high values of porosity, as evidenced from Table 1.

In fact, the density values, which considers the presence of open and closed pores within the matrix, are significantly lower than the values of the pristine powders for the neat PBAT and the different PBAT-based composites, containing GTF and WPL-DH, at different weight percentages.

However, the open porosity is higher compared to the closed one, suggesting that the former has a remarkable role on the printed parts densification the during the sintering process.

It is also possible to note that the porosity percentage of the pure PBAT matrix is lower compared to that of the PBAT-based composites containing GTF.

The values shift from 52 to 56 % and 58 % for the composites loaded with 5 and 10 wt% of maize-wastes filler, respectively. This difference is much more evident for the composites filled with WPL-DH, where the porosity reaches values of 61 and 63 % for the composites containing 5 and 10 wt% of filler deriving from wine production wastes. Moreover, the values of porosity increase with the amount of natural filler

dispersed within the PBAT polymeric matrix [16,17].

Fig. 6 reports the pictures of PBAT (a) and PBAT-based composites objects obtained using SLS, by mixing GTF and WPL-DH powders at different weight percentages, 5 wt% (b) and 10 wt% (c), respectively. The specimens show good dimensional stability revealing a remarkable change of colour due to the presence of increasing concentration of the fillers, which may work as natural colorants and nucleating agents in semi-crystalline polymers, like PBAT.

In fact, the sample's coloration changes from white for the honeycomb hexagon prism realized with the pure PBAT powder, to dark yellow for composites loaded with 10 wt% of GTF. At the same way, the coloration of the specimens containing WPL-DH changes to light grey when the composite was prepared by adding 5 wt% of filler, and finally to dark grey when the filler amount was increased up to 10 wt%. This result put in evidence that the incorporation of biofillers within a polymeric matrix like PBAT negatively affects the densification of the printed parts, by increasing their defectiveness at microscopic level [16,17].

The presence of a high number of pores significantly affects the final resolution of the 3D printed parts in terms of structural integrity and surface finish, making them more exposed to deformation or failure, compromising their final quality. Moreover, during the sintering process, voids can interfere with the distribution of heat within the powder bed, resulting in irregular melting and fusion of the polymeric powder particles, leading to irregularities in the final part's structure and surface finish [28–32]. Furthermore, in some cases, voids can also influence the interaction of the laser with the polymeric powders, causing alterations in the energy absorption and in the subsequent sintering process. This
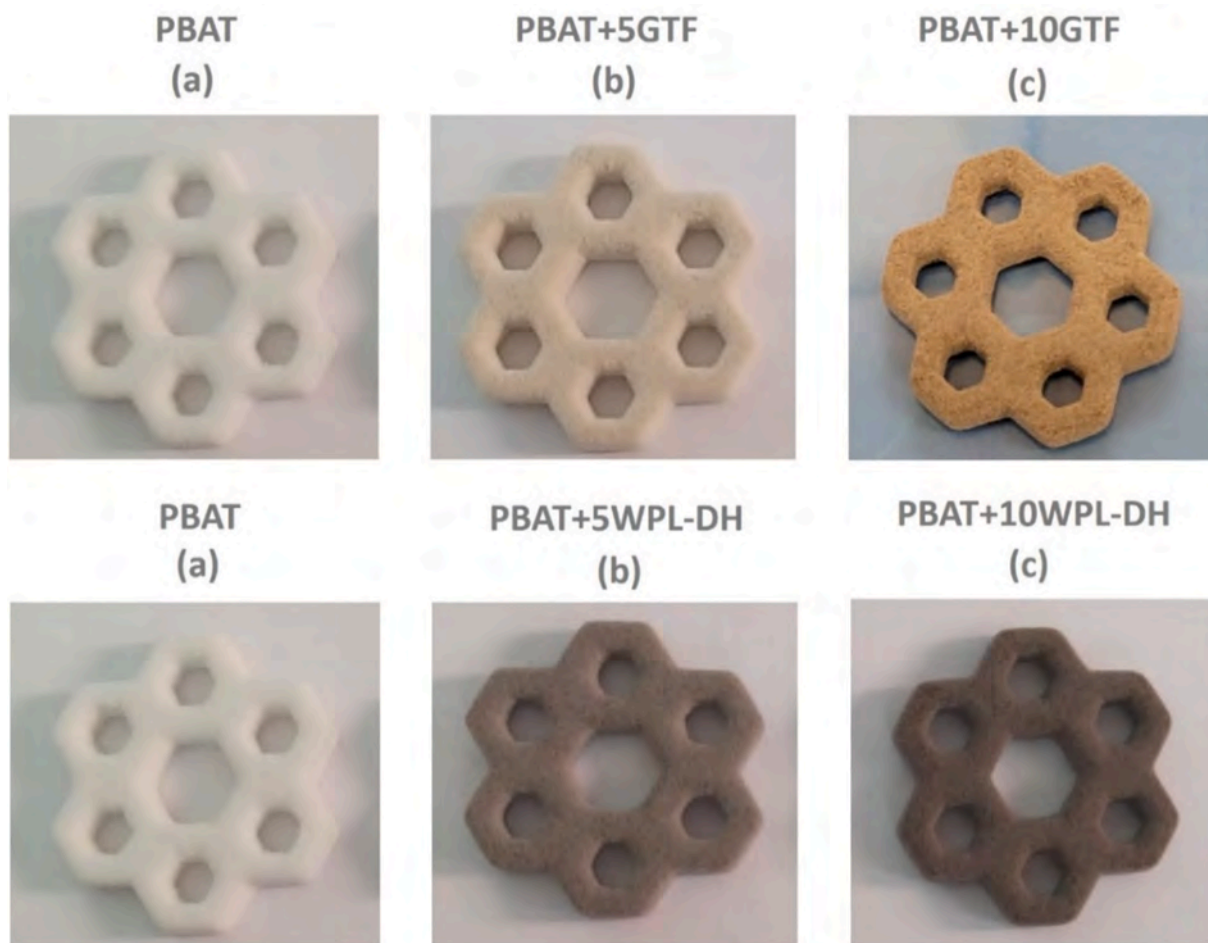
Fig. 6. Top view of 3D printed honeycomb hexagonal prism made of 40 layers of pure PBAT (a) and of bio-based composites containing GTF and WPL-DH at 5 (b) and 10 (c) wt. %, respectively.

can result in a non-uniform melting and consolidation of the powder, that significantly affects the overall resolution and quality of the 3D printed parts.

Minimizing voids can be crucial in SLS to ensure the realization of high-quality parts with the desired resolution, strength, and surface finish. This often involves the optimization of the process parameters, such as laser power, scanning speed, and powder characteristics, as well as ensuring proper powder handling and layering techniques [28–35].

It is possible to affirm that, the values of porosity of the PBAT-based composites, and the possibility to optimize the 3D printing process parameters leading to the realization of specimens with more complex architectures, can enhance in a significant way the use of this polymer in all the fields where high specific porosities are required, such as the biomedical field for the realization of scaffolds and tissues, or for drug
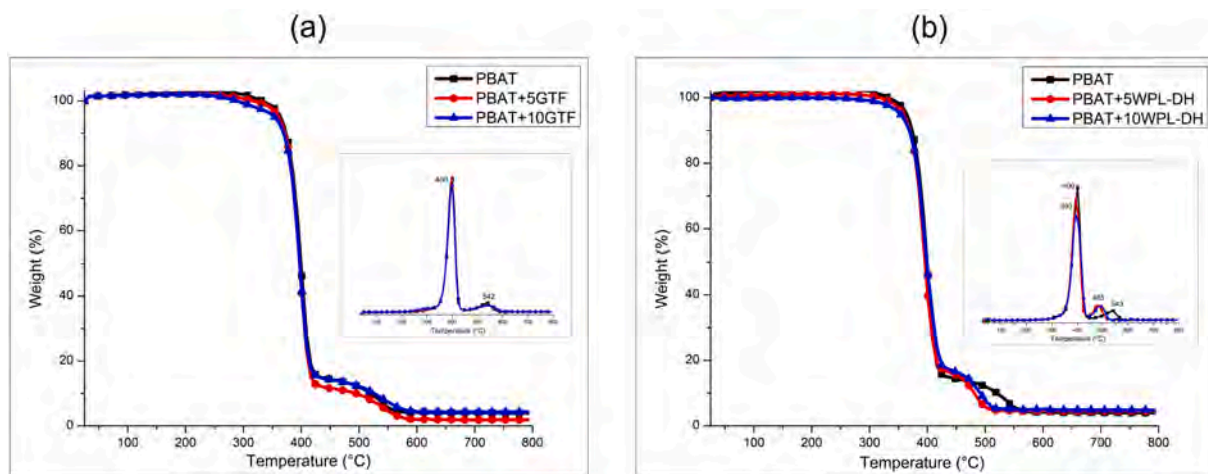
Fig. 7. Thermo-gravimetric curves, performed in air, and related first derivative curves of the neat PBAT and bio-based composites containing GTF (a) and WPL-DH (b), respectively.

release [38–44].

3.4. Thermal analyses of printed bio-based composites

TGA and DSC analyses were carried out to study the thermal properties of PBAT and PBAT-based composites realized by SLS additive manufacturing.

Fig. 7 presents the thermograms and the first derivative curves of the PBAT printed samples compared with the curves related to the bio-based composites obtained by adding the two biofillers, GTF (a) and WPL-DH (b) at different percentages, 5 and 10 wt%, respectively. No significant differences were found in the thermal behavior of both kinds of PBAT-based samples. The presence of the two different biofillers seems to do not affect the final thermal stability of the bio-based composites.

The TG curves of PBAT-based composites are almost the same of the PBAT matrix. In fact, the thermal degradation of PBAT and the bio-based composites occurs in one step with a maximum at 400 °C, corresponding to the complete decomposition of the organic polymer. A small peak also occurs at higher temperatures, and it can be attributed to the char oxidation after the polymeric degradation [34]. The TG curves also evidence the presence of an ash content, close to 2 wt% at 800 °C for all the samples, probably due to the presence of inorganic components within the biofillers composition. This residue is higher for the samples filled with WPL-DH, as previously found in the paragraph related to the powder characterization.

Moreover, DSC analyses were performed to evaluate the melting (T_m), glass transition (T_g), and crystallization (T_c) temperatures, and their enthalpies.

Fig. 8 reports the DSC plots of PBAT, and the composites reinforced with the biofillers coming from different agro-wastes: GTF (a) and WPL-DH (b), respectively.

The neat PBAT shows the typical behavior of a semicrystalline polymer, with a small endothermic peak at around 120 °C, and a Tg value at – 30 °C (during the heating run) correlated to the polymer melting phenomenon, and an exothermic peak at 68 °C (during the cooling run).

The DSC curves of the PBAT-based composites exhibit almost the same behavior of the pure PBAT revealing that the presence of biofillers within the polymeric matrix does not affect the thermal properties of the polymer. The values remain almost the same, independently on the type (GTF or WPL-DH) and amount (5 or 10 wt%) of filler, as reported in Table 2.

However, the crystallinity degree of PBAT, obtained from Equation (6), highlights that the biofillers addition has a significant effect on this parameter [20–22]. In fact, a significant increase in crystallinity can be

observed from 12 % for pristine PBAT up to 24 % for PBAT-based composites containing 10 wt% of GTF. A slight increase of the crystallinity can be also observed for composites filled with WPL-DH as reinforcement, from 12 up to 15 %. This finding can be due to the filler's presence on the surface of PBAT crystals, which promotes a nucleating effect on the polymeric chains, as already reported in the literature for other thermoplastic polymers [45,46].

3.5. Microstructure of printed bio-based PBAT composites

The microstructure of the resulting biodegradable PBAT-composites, obtained using SLS, was investigated by analyzing the composites surface fractures.

Fig. 9 reports few examples of SEM images of PBAT matrix (a) and composites containing 5 wt% of GTF (b) and 10 wt% of WPL-DH (c) biofillers, respectively.

The polymeric particles do not seem well-sintered, as reported in Fig. 9 (a), and this is probably due to the intrinsic characteristics of the biopolymer which contains more amorphous regions (i.e., crystallinity of about 12 % as reported in Table 2), that can cause poor coalescence between particles and poor adhesion among the layers during the printing process.

The composites cross-sections, reported in Fig. 9 (b) and (c), highlight that biofillers are not homogeneously dispersed into the polymer matrix. A phase separation between the fillers and the PBAT powder is evident, which has negative effect on the sintering process, for both kinds of composites. In addition, the low interaction between the polymer and fillers negatively affects the sintering behaviour of the composite powders, [45,46]. As expected, considering the density and the porosity values of the samples, the addition of high percentage of biofillers particles (10 wt%) into the polymeric matrix results in a defective configuration of the parts that become more fragile to handle compared to the 5 wt% counterparts, making them not practical to be used for SLS applications [47,48]. This could represent the reason why the composites mechanical properties decrease with high percentages of filler, as also known from the literature [16,17].

3.6. Dynamic mechanical analysis of printed bio-based PBAT composites

The dynamo-mechanical curves are reported in Fig. 10 for the different bio-based specimens. The storage modulus (E') and tan δ values were evaluated considering the high values of porosity typical of these samples. Fig. 10 (a) shows the elastic modulus of the composites reinforced with biofillers deriving from wine wastes. As visible, in the glassy region at −40 °C, the storage modulus of 5 wt% filled samples is
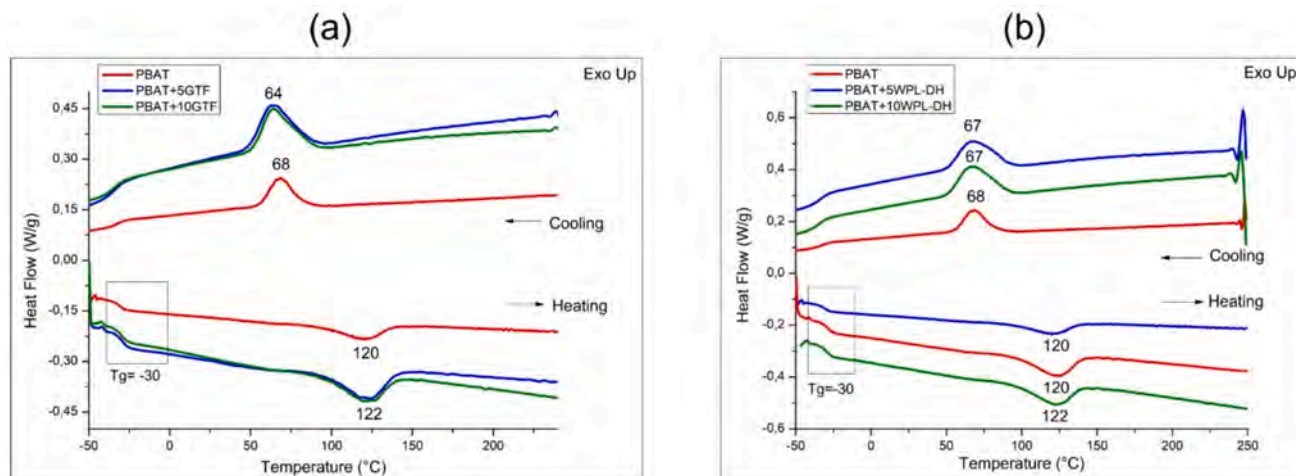

Fig. 8. DSC curves, collected under nitrogen, of the neat PBAT and of the bio-based composites containing different biofillers: GTF (a) and WPL-DH (b), respectively.
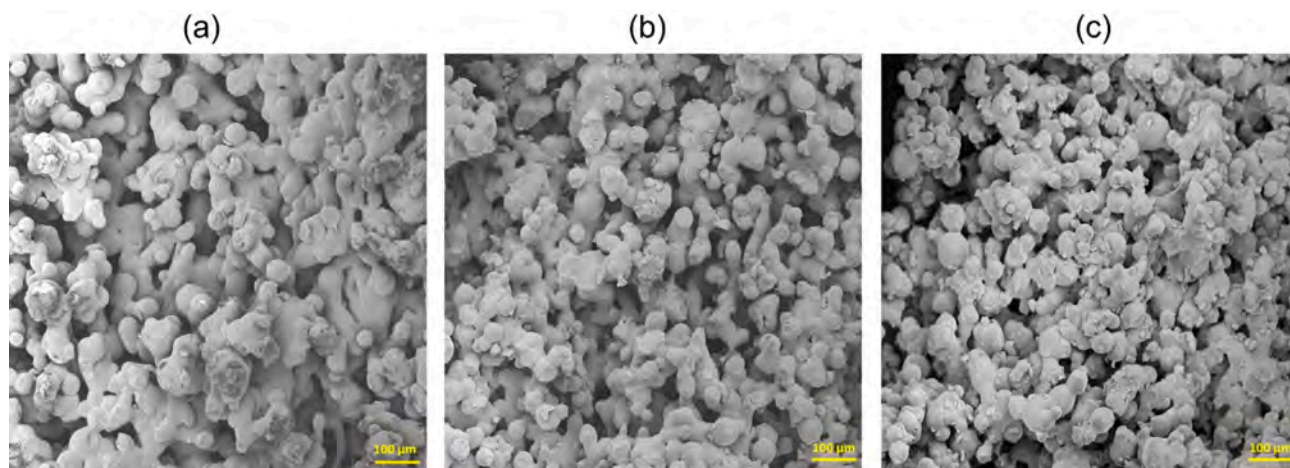
Fig. 9. SEM micrographs, at 300X, of sintered PBAT matrix (a) and PBAT-based composites with 5 wt% of GTF (b) and 10 wt% of WPL-DH (c).
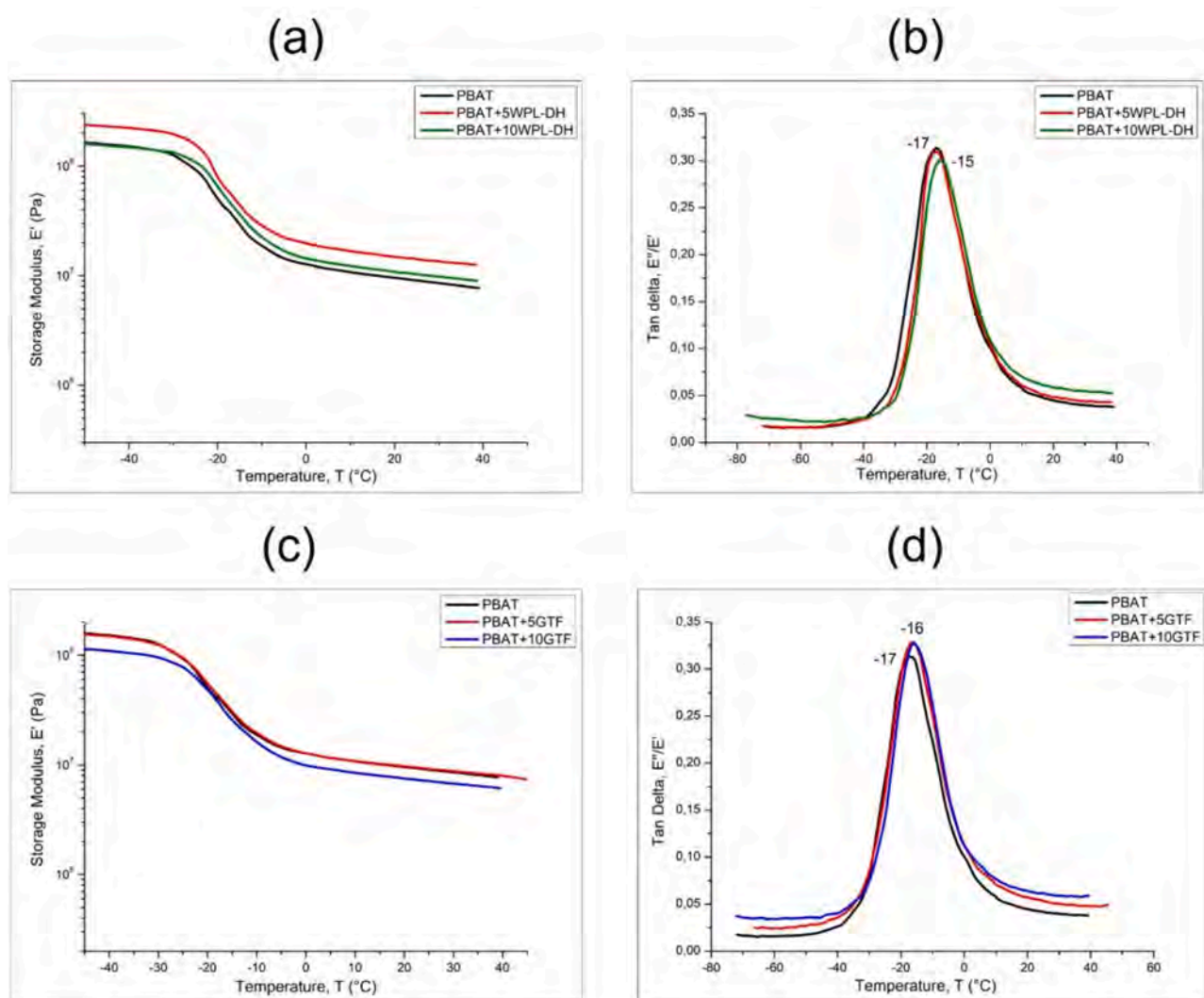

Fig. 10. DMA curves of the neat PBAT and bio-based composites containing different weight percentages of WPL-DH (a, b) and GTF (c, d), respectively.

higher than that of neat PBAT. This increase is significant taking into account the higher porosity (61 %) of the composite respect to the un-filled polymer (52 %). The storage modulus values, related to the elastic component, shift from 153 MPa to 224 MPa for PBAT + 5WPL-DH.

This enhancement could be associated to the stiffening effect induced by the presence of the WPL-DH particles, which limits the polymeric molecular chains mobility [48,49]. Thus, the polymer flow is restricted, and the bio-based composites remain stiffer.

However, the storage modulus values do not follow the same increment by increasing the filler content up to 10 wt%. This decrease can be probably joined to the low interfacial interaction between polymer and fillers, and poor adhesion of the layers occurred during the sintering process [17,45,46]. The same behaviour has been observed for the PBAT-based composites loaded with the filler obtained from wastes of corn agricultural industry.

The presence of higher percentages of GTF leads to a reduction of the storage modulus values, as reported in Fig. 9 to indicate the negative effects of the poor interaction of the filler with the PBAT matrix for these kinds of composites and, above all, the presence of high number of pores. In fact, an increase in void and pores content put in evidence a lower adhesion of the layers during the 3D printing process for the composites containing higher percentages of biofillers and, consequently, changes in their final mechanical properties.

The pores content significantly raises by increasing the concentration of biofillers particles up to 10 wt% [45,46], as revealed by the higher values of porosity of the 3D printed samples (see Table 1).

Dynamic-mechanical results, listed in Table 3, clearly indicate that a good interaction between filler and matrix can be reached by adding 5 wt% of the two kinds of biofillers. Moreover, DMA analysis put in evidence an insignificant variation of the glass transition temperature values for PBAT-based composites compared with the matrix, as visible from tan delta curves as function of temperature reported in Fig. 10 (b) for WPL-DH and (d) for GTF, respectively.

Tg values slightly shift from -17 °C for the pure polymer to -15 °C for the composites filled with 10 wt% of GTF. As evident, Tg values obtained from DMA analyses (-15 °C) greatly differ from the values obtained by performing DSC analyses (-30 °C). This difference is well-known from the literature, and it can be assigned to the different characterization techniques [50].

Summing up the results obtained in this work, we can say that the use of these kinds of biofillers for the preparation of PBAT-based composites can reduce the environmental issue and costs, but also lead to several benefits in particular in those applications where the presence of porosities is strictly desired, such as the preparation of scaffolds or tissues [36–41] for biomedical applications.

3.7. Cytocompatibility tests

A preliminary study on the cytocompatibility of the PBAT matrix and PBAT-based composites was performed to assess the capability of the printed samples to determine possible cytotoxic events resulting from the release of compounds from the neat PBAT and the composite filled with the two different agro-wastes, at different concentrations. No cytotoxic effects were observed through indirect tests revealing that the PBAT-based samples do not induce cell death by the release of traces of photoinitiator, unreacted monomers or degradation products within the first day (conditioned medium_1 d) [51,52]. The percentages of viable cells were reported in Fig. 11.

No significant differences in the cell viability were found among the samples loaded with the two different biofillers and filler contents, compared with the CNTR, as visible from Fig. 11. The biofillers addition does not affect cell adhesion and proliferation, although a slight reduction in cell number was observed for the samples loaded with WPL-DH biofillers compared to the control, probably due to its chemical composition [51]. Surely, further studies are necessary to better understand the cytotoxicity of these new systems even doing direct tests to investigate cell adhesion and proliferation, at the different time points.

4. Conclusions

PBAT can be considered a very promising biodegradable polymers. This study demonstrated that PBAT-based composites reinforced with biofillers deriving from agro-wastes, can be processed by selective laser sintering. Printed parts were successfully realized after mixing PBAT
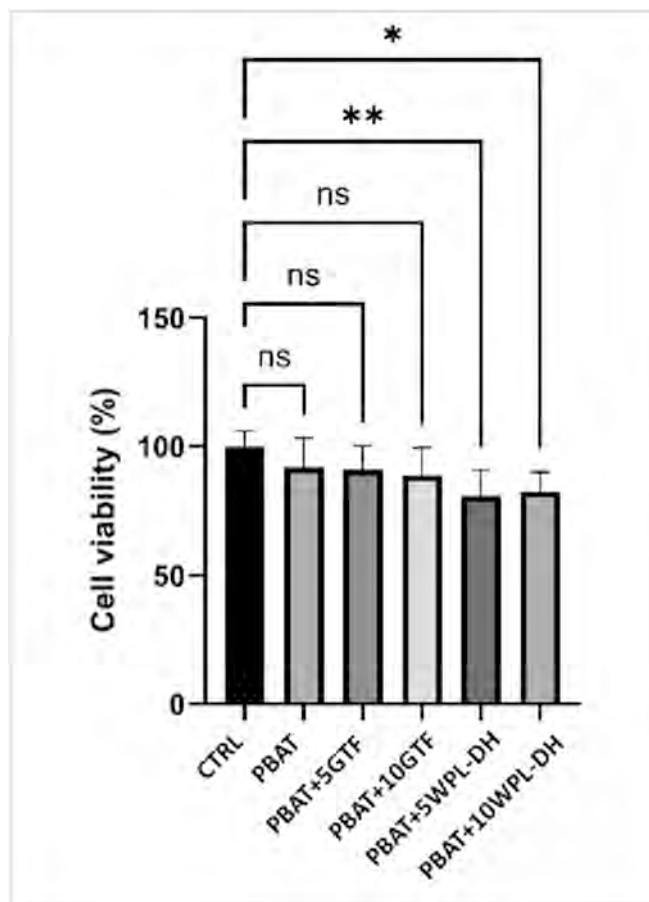
Fig. 11. HFF-1 cell viability performed by indirect tests where samples were soaked for 24 h (conditioned medium for 24 h).

microspheres with particles of GTF, a yellow powder obtained from corn wastes, and WPL-DH, a grey powder obtained from wastes of wine production.

The PBAT-based composites filled with the agro-wastes powders showed inhomogeneous dispersion of the fillers within the polymeric matrix through a simple and greener approach, such as mechanical mixing. The specimens obtained by SLS show good dimensional geometry, good level of details with full and empty spaces, without evident defects, and high values of porosity, ideal for applications in biomedical field.

The addition of the biofillers within the PBAT matrix leads to a crystallinity increase of the PBAT-based composites because the presence of natural particles promotes a nucleating effect on the polymeric chains. Moreover, the addition of the fillers at lower weight percentages (5 wt%) allows to obtain an increase of the modulus value for the composites compared to the pure PBAT.

On the contrary, higher amount of biofillers has remarkable effect on the porosity of the final composites, which significantly enhances because of the presence of a high number of voids, that negatively affect the final mechanical properties of the biodegradable composites, influencing the layers adhesion during the sintering process.

The results obtained and the above discussion enable to say that PBAT and its bio-based composites can offer a valid alternative to the conventional polymers, in terms of environmental and economic aspects. However, there is a need for more studies to make these kinds of materials competitive, increasing their use for many industrial applications. Biocompatibility and cytotoxicity should be also investigated in detail in order to effectively applied the PBAT-based composites to biomedical field together with their porosity and flexibility. Many

challenges remain to overcome as well as the opportunity to improve the composites mechanical performances, and to allow their industrial-scale preparation.

CRediT authorship contribution statement

Giovanna Colucci: Writing – review & editing, Writing – original draft, Visualization, Validation, Supervision, Methodology, Investigation, Formal analysis, Data curation, Conceptualization. **Federico Lupone:** Writing – original draft, Investigation, Data curation. **Federica Bondioli:** Supervision, Resources, Project administration, Funding acquisition. **Massimo Messori:** Supervision, Resources, Project administration, Funding acquisition.

Declaration of competing interest

The authors declare that they have no known competing financial interests or personal relationships that could have appeared to influence the work reported in this paper.

Data availability

Data will be made available on request.

References

[1] K. Van de Velde, P. Kiekens, Biopolymers: overview of several properties and consequences on their applications, Polym. Test. 21 (4) (2002) 433–442.

[2] R. Balart, D. Garcia-Garcia, V. Fombuena, L. Quiles-Carrillo, M.P. Arrieta, Biopolymers from natural resources, Polymers 13 (2021) 2532, https://doi.org/10.3390/polym13152532.

[3] R.P. Babu, K' O'Connor, Ramakrishna Seeram, Current progress on bio-based polymers and their future trends, Prog. Biomater. 2 (2013) 8, https://doi.org/10.1186/2194-0517-2-8.

[4] V.K. Thakur, A.S. Singha, M.K. Thakur, Biopolymers based green composites: mechanical thermal and physico-chemical characterization, J Polym. Environ. 20 (2012) 412–421, https://doi.org/10.1007/s10924-011-0389-y.

[5] A.K. Mohanty, M. Misra, L.T. Drzal, Sustainable Bio-Composites from Renewable Resources: Opportunities and Challenges in the Green Materials World, J. Polym. Environ. 10 (2002) 19–26.

[6] J. Zhang, V. Hirschberg, D. Rodrigue, Mechanical fatigue of biodegradable polymers: a study on polylactic acid (PLA), polybutylene succinate (PBS) and polybutylene adipate terephthalate (PBAT), International Journal of Fatigue 159 (2022) 106798, https://doi.org/10.1016/j.ijfatigue.2022.106798.

[7] S. Ayu Rafiqah, A. Khalina, A. Saffian Harmaen, I. Amin Tawakkal, K. Zaman, M. Asim, M.N. Nurrazi, C.H. Lee, A review on properties and application of bio-based poly (butylene succinate), Polymers 13 (2021) 1436, https://doi.org/10.3390/polym13091436.

[8] Y.-X. Weng, Y.-J. Jin, Q.-Y. Meng, L. Wang, M. Zhang, Y.-Z. Wang, Biodegradation behavior of poly(butylene adipate-coterephthalate) (PBAT), poly(lactic acid) (PLA), and their blend under soil conditions, Polymer Testing 32 (2013) 918–926.

[9] K.M. Nampoothiri, N.R. Nair, R.P. John, An overview of the recent developments in polylactide (PLA) research, Biores. Technol. 101 (2010) 8493–8501.

[10] C. Sciancalepore, E. Togliatti, A. Giubilini, D. Pugliese, M. Fabrizio Moroni, D. M. Messori, Preparation and characterization of innovative poly (butylene adipate terephthalate)-based biocomposites for agri-food packaging application, J Appl Polym Sci. 139 (2022) 52370–52387, https://doi.org/10.1002/app.52370.

[11] Z.U. Arif, M.Y. Khalid, Novel biopolymer-based sustainable composites for food packaging applications: a narrative review, Food Packag. Shelf Life (2022) 33, https://doi.org/10.1016/j.fpsl.2022.100892.

[12] J. Baranwal, B. Barse, A. Fais, G.L. Delogu, A. Kumar, Biopolymer: a sustainable material for food and medical applications, Polymers (2022) 14, https://doi.org/10.3390/polym14050983.

[13] F.V. Ferreira, L.S. Cividanes, R.F. Gouveia, L.M.F. Lona, An overview on properties and applications of poly (butylene adipate-co-terephthalate)-PBAT based composites, Polym. Eng. Sci. 59 (2019) 7–15, https://doi.org/10.1002/pen.24770.

[14] H. Kargarzadeh, A. Galeski, A. Pawlak, PBAT green composites: Effects of kraft lignin particles on the morphological, thermal, crystalline, macro and micromechanical properties, Polymer 203 (2020) 122748, https://doi.org/10.1016/j.polymer.2020.122748.

[15] N.P. Sunesh, S. Indran, D. Divya, S. Suchart, Isolation and characterization of novel agrowaste-based cellulosic micro fillers from Borassus flabellifer flower for polymer composite reinforcement, Polym. Compos. 43 (2022) 6476–6488, https://doi.org/10.1016/j.heliyon.2023.e17760.

[16] N.B. Arzumanova, N.T. Kakhramanov, Polymer biocomposites based on agro waste: part II husk, stalk and straw of some agricultural crops as dispersed filler, new materials, Compounds Appl. 4 (2020) 153–172.

[17] N.B. Arzumanova, Polymer biocomposites based on agro waste: part III shells of various nuts as natural filler for polymer composites, new materials, Compounds Appl. 5 (2021) 19–44, https://doi.org/10.1016/j.matdes.2009.01.009.

[18] Chi-Hui Tsou, Zhi-Jun Chen, Shuai Yuan, Zheng-Lu Ma, Chin-San Wu, Tao Yang, Chun-Fen Jia, M.R. De Guzman, The preparation and performance of poly (butylene adipate) terephthalate/corn stalk composites, Current Res. Green Sustain. Chem. (2022) 5, 100329. doi.org/10.1016/j.crgsc.2022.100329.

[19] H. Moustafa, C. Guizani, A. Dufresne, Sustainable biodegradable coffee grounds filler and its effect on the hydrophobicity, mechanical and thermal properties of biodegradable PBAT composites, J. Appl. Polym. Sci. (2016) 44498–44508, https://doi.org/10.1002/APP.44498.

[20] L. Botta, V. Titone, M.C. Mistretta, F.P. La Mantia, A. Modica, M. Bruno, F. Sottile, F. Lopresti, PBAT based composites reinforced with microcrystalline cellulose obtained from softwood almond shells, Polymers 13 (2021) 2643, https://doi.org/10.3390/polym13162643.

[21] S. Berretta, O. Ghita, K.E. Evans, Morphology of polymeric powders in Laser Sintering (LS): From Polyamide to new PEEK powders, Eur. Polym. J. 59 (2014) 218–229.

[22] K. Fukushima, M.H. Wu, S. Bocchini, A. Rasyida, M.C. Yang, PBAT based nanocomposites for medical and industrial applications, Mater. Sci. Eng. C 32 (2012) 1331–1351.

[23] S.S. Alghamdi, S. John, N. Roy Choudhury, N.K. Dutta, Additive manufacturing of polymer materials: progress, promise and challenges, Polymers 13 (2021) 753–791, https://doi.org/10.3390/polym13050753.

[24] N. Li, D. Qiao, S. Zhao, Q. Lin, B. Zhang, F. Xie, 3D printing to innovate biopolymer materials for demanding applications: a review, Mater. Today Chem. 20 (2021) 100459, https://doi.org/10.1016/j.mtchem.2021.100459.

[25] C.M. Thakar, S. S. Parkhe, A. Jain, K.t Phasinam, G. Murugesan, R. Joy M. Ventayen, 3D Printing: Basic principles and applications, Mater. Today Proc. (2022) 51, 842–849. doi.org/10.1016/j.matpr.2021.06.272.

[26] A. Jandyal, I. Chaturvedi, I. Wazir, A. Raina, Mir Irfan Ul Haq, 3D printing –A review of processes, materials, and applications in industry 4.0, Sustain. Oper. Comput. 3 (2022) 33–42, https://doi.org/10.1016/j.susoc.2021.09.004.

[27] M. Khorram Niaki, F. Nonino, G. Palombi, S.A. Torabi, Economic sustainability of additive manufacturing, J. Manuf. Technol. Manage. 30 (2019) 353–365, https://doi.org/10.1108/JMTM-05-2018-0131.

[28] T. Pepelnjak, J. Stojšic, L. Sevšek, D. Movrin, M. Milutinovic, Influence of process parameters on the characteristics of additively manufactured parts made from advanced biopolymers, Polymers 15 (2023) 716, https://doi.org/10.3390/polym15030716.

[29] L.J. Tan, Wei Zhu, Kun Zhou, Recent Progress on Polymer Materials for Additive Manufacturing, Adv. Function. Mater. (2020) 30, 2003062-2003115. doi: 10.1002/adfm.202003062.

[30] Y. Wang, Z. Xu, Wu. Dingdi, J. Bai, Current status and prospects of polymer powder 3D printing technologies, Materials 13 (2020) 2406, https://doi.org/10.3390/ma13102406.

[31] F. Lupone, E. Padovano, M. Pietroluongo, S. Giudice, O. Ostrovskaya, C. Badini, Optimization of selective laser sintering process conditions using stable sintering region approach, Express Polym. Lett. 15 (2) (2021) 77–192, https://doi.org/10.3144/expresspolymlett.2021.16.

[32] J. Schmidt, M. Sachs, C. Blumel, B. Winzer, F. Toni, K.E. Wirth, W. Peukert, A novel process chain for the production of spherical SLS polymer powders with good flowability, Proc. Eng. 102 (2015) 550–556, https://doi.org/10.1016/j.proeng.2015.01.123.

[33] R.G. Kleijnen, Manfred Schmid and Konrad Wegener. Production and processing of a spherical polybutylene terephthalate powder for laser sintering, Appl. Sci. (2019) 9 (7), 1308–1324. doi:10.3390/app9071308.

[34] G. Colucci, M. Piano, F. Lupone, C. Badini, F. Bondioli, M. Messori, Preparation and 3D printability study of biobased PBAT powder for selective laser sintering additive manufacturing, Mater. Today Chem. 33 (2023) 101687, https://doi.org/10.1016/j.mtchem.2023.101687.

[35] B.O. Sivadas, I. Ashcroft, A.N. Khlobystov, R.D. Goodridge, Laser sintering of polymer nanocomposites, Adv. Ind. Eng. Polym. Res. 4 (2021) 277–300, https://doi.org/10.1016/j.aiepr.2021.07.003.

[36] R. Arrigo, A. Frache, FDM printability of PLA based-materials: the key role of the rheological behavior, Polymers 14 (2022) 1754.

[37] B. Haworth, N. Hopkinson, D. Hitt, X. Zhong, Shear viscosity measurements on Polyamide-12 polymers for laser sintering, Rapid Prototyp. J. 19 (1) (2013) 28–36.

[38] J. Jian, Z. Xiangbin, H. Xianbo, An overview on synthesis, properties and applications of poly (butylene-adipate-co-terephthalate)-PBAT, Adv. Ind. Eng. Polym. Res. 3 (2020) 19–26, https://doi.org/10.1016/j.aiepr.2020.01.00.1.

[39] C.M. González-Henríquez, M.A. Sarabia-Vallejosc, J. Rodriguez-Hernandez, Polymers for additive manufacturing and 4D-printing: Materials, methodologies, and biomedical applications, Prog. Polym. Sci. 94 (2019) 57–116, https://doi.org/10.1016/j.progpolymsci.2019.03.001.

[40] D.W. Hutmacher, Scaffolds in tissue engineering bone and cartilage, Biomaterials 21 (2000) 2529–2543, https://doi.org/10.1016/s0142-9612(00)00121-6.

[41] S.W. Qiu, Y.H. Xia, J.D. Sun, S.S. Wang, Q.S. Xing, Poly (butylene adipate-co-terephthalate)/Sodium alginate blends have superior characteristics and can be used to fabricate vascular stents, Mater. Res. Express 9 (5) (2022) 55401–55410.

[42] S. Bose, S. Vahabzadeh, A. Bandyopadhyay, Bone tissue engineering using 3D printing, Materials Today 16 (2013) 496–504, https://doi.org/10.1016/j.mattod.2013.11.017.

[43] M. Karimi, A. Asefnejad, D. Aflaki, A. Surendar, H. Baharifar, S. Saber-Samandari, A. Khandan Afrasyab Khan, D. Toghraie, Fabrication of shapeless scaffolds reinforced with baghdadite-magnetite nanoparticles using a 3D printer and freeze-drying technique, J. Mater. Res. Technol. 14 (2021) 3070–3079, https://doi.org/10.1016/j.jmrt.2021.08.084.

[44] P. Iranmanesh, A. Ehsani, A. Khademi, A. Asefnejad, S. Shahriari, M. Soleimani, M. Ghadiri Nejad, S. Saber-Samandari, A. Khandan, Application of 3D bioprinters for dental pulp regeneration and tissue engineering (Porous architecture), Transport Porous Media 142 (2022) 265–293, https://doi.org/10.1007/s11242-021-01618-x.

[45] P. Svoboda, M. Dvorackova, D. Svobodova, Influence of biodegradation on crystallization of poly (butylene adipate-co-terephthalate), Polym Adv Technol. 30 (2019) 552–562, https://doi.org/10.1002/pat.4491.

[46] Y. Kong, J.N. Hay, The measurement of the crystallinity of polymers by DSC, Polymers 43 (2002) 3873–3878.

[47] K. Senthilkumaran, P.M. Pandey, P.V.M. Rao, Influence of building strategies on the accuracy of parts in selective laser sintering, Materials and Design 30 (2009) 2946–2954, https://doi.org/10.1016/j.matdes.2009.01.009.

[48] Y. Shi, Z. Li, H. Sun, S. Huang, F. Zeng, Effect of properties of polymer materials on the quality of selective laser sintering parts, J Mater Des Appl 218 (2004) 247–252, https://doi.org/10.1177/146442070421800308.

[49] E. Togliatti, D. Pugliese, A. Giubilini, M. Messori, D. Milanese, C. Sciancalepore, Novel PBAT-based biocomposites reinforced with bioresorbable phosphate glass microparticles, Macromol. Symp. 405 (2022) 2100238, https://doi.org/10.1002/masy.202100238.

[50] C.A. Gracia-Fernandez, S. Gómez-Barreiro, J. López-Beceiro, J. Tarrío Saavedra, S. Naya, R. Artiaga, Comparative study of the dynamic glass transition temperature by DMA and TMDSC, Polymer testing, (2010). doi: 10.1016/j.polymertesting.2010.09.005.

[51] C. Tonda-Turo, I. Carmagnola, A. Chiappone, Z. Feng, G. Ciardelli, M. Hakkarainen, M. Sangermano, Photocurable chitosan as bioink for cellularized therapies towards personalized scaffold architecture, Bioprinting 18 (2020) e00082.

[52] G. Melilli, I. Carmagnola, F. Chiara Tonda-Turo, G. Pirri, M. Ciardelli, M. Sangermano, A.C. Hakkarainen, DLP 3D printing meets lignocellulosic biopolymers: carboxymethyl cellulose inks for 3D biocompatible hydrogels, Polymers 12 (2020) 1655, https://doi.org/10.3390/polym12081655.